Developmental Cell, Vol. 7, 117–123, July, 2004, Copyright ©2004 by Cell Press

Semaphorin-Plexin Signaling Guides Patterning of the Developing Vasculature

Short Article

Jesús Torres-Vázquez,[1,5] Aaron D. Gitler,[2,5] Sherri D. Fraser,[3,5] Jason D. Berk,[1] Van N. Pham,[1] Mark C. Fishman,[4,7] Sarah Childs,[3,6] Jonathan A. Epstein,[2,6] and Brant M. Weinstein[1,6,*]

[1]Laboratory of Molecular Genetics
NICHD
National Institutes of Health
Bethesda, Maryland 20892

[2]Cardiovascular Division
University of Pennsylvania
Philadelphia, Pennsylvania 19104

[3]Department of Biochemistry and Molecular Biology and Smooth Muscle Research Group
University of Calgary
Calgary, Alberta T2N 4N1
Canada

[4]Cardiovascular Research Center
Massachusetts General Hospital
Charlestown, Massachusetts 02129

Summary

Major vessels of the vertebrate circulatory system display evolutionarily conserved and reproducible anatomy, but the cues guiding this stereotypic patterning remain obscure. In the nervous system, axonal pathways are shaped by repulsive cues provided by ligands of the semaphorin family that are sensed by migrating neuronal growth cones through plexin receptors. We show that proper blood vessel pathfinding requires the endothelial receptor PlexinD1 and semaphorin signals, and we identify mutations in *plexinD1* in the zebrafish vascular patterning mutant *out of bounds*. These results reveal the fundamental conservation of repulsive patterning mechanisms between axonal migration in the central nervous system and vascular endothelium during angiogenesis.

Introduction

The vertebrate circulatory system is crucial for the delivery and exchange of gases, hormones, metabolic wastes, and immunity factors. Although key players in vascular endothelial cell specification and differentiation have been identified, we have limited understanding of the molecular mechanisms responsible for the remarkable regularity in pattern of larger blood vessels within and across species (Weinstein, 1999). In the nervous system, axonal pathways are established by repulsive and attractive signals from surrounding tissues, sensed by migrating neuronal growth cones through specific receptors (Tessier-Lavigne and Goodman, 1996). The semaphorin family of ligands and their plexin receptors are key players in neuronal pathfinding. Semaphorins inhibit migration of plexin-expressing neuronal growth cones, restricting their navigation pathways (Tamagnone and Comoglio, 2000). We show here that the endothelial receptor PlexinD1 plays a similar role during vascular patterning. In the developing trunk, angiogenic intersegmental vessels extend near somite boundaries (Isogai et al., 2001; Childs et al., 2002). Loss of *plxnD1* function via morpholino injection or in zebrafish *out of bounds (obd)* mutants (Childs et al., 2002) causes dramatic mispatterning of these vessels, which are no longer restricted to growth near intersomitic boundaries. Somites flanking intersegmental vessels express semaphorins (Roos et al., 1999; Yee et al., 1999), and reducing the function of these semaphorins causes similar intersegmental vessel patterning defects. Conversely, semaphorin overexpression inhibits the growth of intersegmental vessels in a *plxnD1*-dependent manner. These results indicate that the establishment of anatomical pattern in the developing vasculature is directed in part by cues and mechanisms similar to those used to pattern the developing nervous system (Tessier-Lavigne and Goodman, 1996), including semaphorin-plexin signaling.

Results and Discussion

Plexin D1 Is Expressed in the Embryonic Vasculature

We identified murine *plexinD1 (plxnD1)* in the EST database by sequence homology to other members of the plexin family. Expression analysis revealed that *plxnD1*, unlike other members of the extended family, is not primarily expressed by neurons. Rather, expression is restricted to endothelial cells (Cheng et al., 2001; Tamagnone et al., 1999; van der Zwaag et al., 2002). We reasoned that *plxnD1* might function to guide the patterning of developing blood vessels, in a manner analogous to the role of other plexins in axonal patterning in the nervous system (Tamagnone and Comoglio, 2000). To explore this possibility, we isolated a full-length zebrafish *plxnD1* ortholog (see Experimental Procedures and Supplemental Data, section 1 [http://www.developmentalcell.com/cgi/content/full/7/1/117/DC1]). Zebrafish *plxnD1* is expressed throughout the vasculature in blood vessel endothelial cells and their angioblast precursors (Figures 1B, 1D, 1F, and 1H), mirroring the endothelial-specific expression pattern of the *fli1* gene (Figures 1A, 1C, 1E, and 1G; Brown et al., 2000). *plxnD1* transcripts are evident in angioblast precursors prior to trunk vessel assembly (Figure 1B) and in the newly formed trunk dorsal aorta and posterior cardinal vein (Figure 1D). These two vessels form via vasculogenesis, or the coalescence of migratory angioblast precursor cells originating in the lateral mesoderm to form cellular cords, and then open vessels (Risau and Flamme, 1995).

*Correspondence: bw96w@nih.gov

[5]These authors contributed equally to this work.

[6]These authors contributed equally to this work.

[7]Present address: Novartis Institutes for Biomedical Research, Cambridge, Massachusetts 02139.

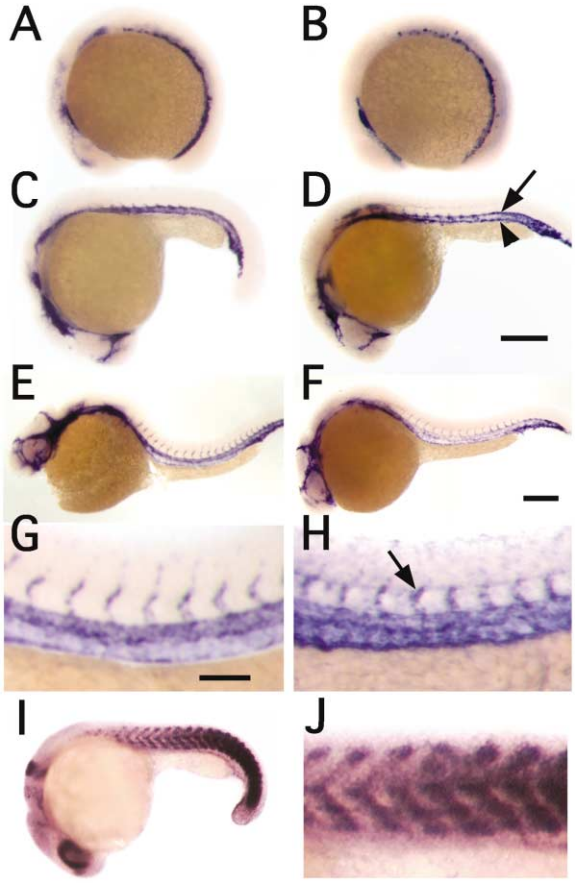

Figure 1. PlexinD1 Is Expressed in the Vasculature during Zebrafish Vascular Development

Whole-mount in situ hybridization reveals similar expression patterns of *fli1* (A, C, E, and G) and *plxnD1* (B, D, F, and H) mRNA in approximately 13–14 hpf (A and B), 19–20 hpf (C and D), and 27 hpf ([E] and [F], insets magnified in [G] and [H]) zebrafish. Transcription of *sema3a2* at 19–20 hpf ([I], inset magnified in [J]) prefigures the areas avoided by migrating zebrafish intersegmental vessels. Lateral views, anterior to the left. The arrow and arrowhead in (D) point to the dorsal aorta and cardinal vein, respectively. The arrow in (H) points to an intersegmental vessel sprout. Scale bars = 200 μm (A, B, C, D, and I), 200 μm (E and F), and 100 μm (G, H, and J).

Zebrafish *plxnD1* is also expressed in the metamerically repeating intersegmental vessels that sprout from the dorsal aorta adjacent to intersomitic boundaries at a slightly later point in development (Figures 1F and 1H; Isogai et al., 2001; Childs et al., 2002). The intersegmental vessels form via angiogenesis, or the emergence and elongation of new vessels from preexisting vessels (Risau and Flamme, 1995).

plxnD1 Morphants Display Intersegmental Vessel Patterning Defects

To investigate the function of *plxnD1* in the zebrafish vasculature, we used antisense morpholino oligonucleotides (morpholinos) to prevent correct splicing (Draper et al., 2001) of two separate exons of the immature *plxnD1* mRNA message in vivo. *plxnD1* splicing morpholinos (*plxnD1*$^{2215\text{-}2304}$ and *plxnD1*$^{3207\text{-}3462}$) or control morpholinos were injected separately into one-cell to four-cell *TG(fli1:EGFP)*^{y1} embryos. *TG(fli1:EGFP)*^{y1} zebrafish carry an endothelial-specific EGFP reporter that enables detailed visualization of developing blood vessels in vivo (Lawson and Weinstein, 2002). Embryos injected with control morpholinos (control morphants) display endothelial behavior and patterning indistinguishable from that of untreated *TG(fli1:EGFP)*^{y1} embryos (Figures 2A, 2C, 2F, and 2H). In the trunk, the axial dorsal aorta and posterior cardinal vein assemble at 16.5–18 hr postfertilization (hpf) and begin to carry circulation by 24–26 hpf. Intersegmental vessel sprouts emerge bilaterally from the dorsal aorta at approximately 20 hpf. Nascent intersegmental vessels grow dorsally close to intersomitic boundaries (Figures 2A and 2C and Supplemental Movie S1[http://developmentalcell.com/cgi/content/full/7/1/117/DC1]). They extend through the spaces between the somites and the notochord or somites and neural tube but do not penetrate into these tissues (Figures 2E and 2F). By 30–35 hpf, the fully extended intersegmental vessels on each side of the embryo interconnect above the neural tube to form two paired dorsal longitudinal anastomotic vessels (DLAV, Figure 2C; Isogai et al., 2001).

The two *plxnD1* splicing morpholinos (*plxnD1*$^{2215\text{-}2304}$ and *plxnD1*$^{3207\text{-}3462}$) strongly reduce the levels of correctly spliced *plxnD1* mRNA (see Supplemental Data, section 2) and elicit very similar dramatic defects in trunk vascular patterning. The dorsal aorta and posterior cardinal vein assemble normally in *plxnD1* morphants, but the intersegmental vessels are highly abnormal. Intersegmental vessel sprouts emerge from the dorsal aorta at irregular positions (Figure 2B and Supplemental Movie S2), and the elongating sprouts do not track close to intersegmental boundaries, instead forming complex and highly branched interconnecting patterns along the trunk (Figure 2D and Supplemental Movie S2). Misguided sprouts fail to observe normal anteroposterior boundaries in *plxnD1* morphants, but they do avoid penetrating into the somites and other adjacent tissues (Figures 2E–2G). The misguidance defects are more severe in the ventral trunk, with no obvious defects in the DLAV. We also visualized endothelial cell nuclei and cell shapes in wild-type embryos and *plxnD1* morphants derived from *fli:nEGFP* transgenic fish (unpublished data). This analysis indicated that aberrant pathfinding behavior, rather than increased numbers of endothelial cells, accounts for the *plxnD1* vascular mispatterning phenotype. By 3 dpf, most of the aberrant trunk vessels in *plxnD1* morphants develop into functional lumenized vessels carrying circulatory flow (Figure 2I), albeit in highly abnormal patterns (see Supplemental Movies S3–S5). Although the trunk axial vessels form normally, the remodeling of the caudal vein sinus is abnormal in *plxnD1* morphants. These vessels do still carry circulatory flow, however. The lack of trunk axial vessel defects suggests that loss of *plxnD1* function does not affect endothelial specification or arterial-venous identity. To confirm this, we performed whole-mount RNA in situ hybridization on 24 hpf *plxnD1* morphants using the pan-endothelial marker *tie-1* (Lyons et al., 1998), as well as riboprobes specific for *ephrinB2* and *ephB4* (Lawson et

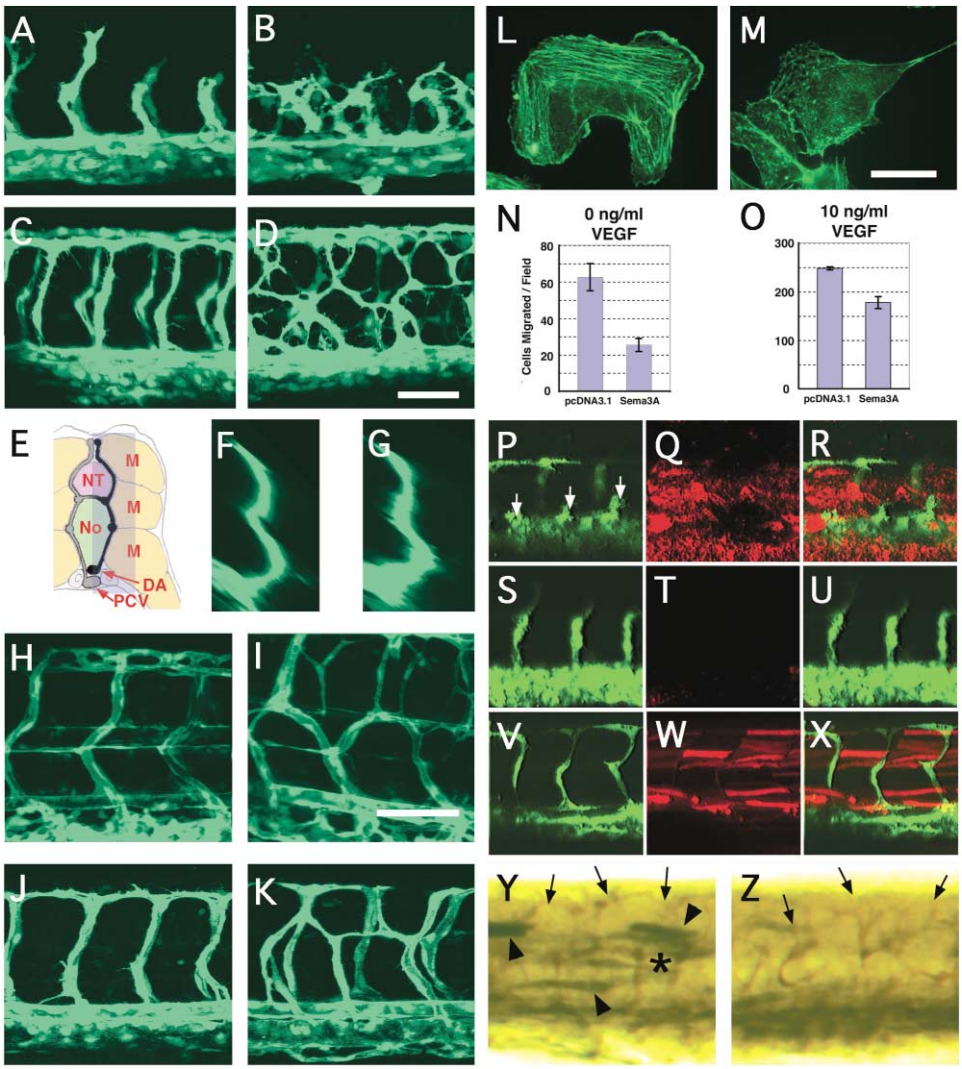

Figure 2. PlexinD1 and Semaphorins Are Required for Proper Patterning of Trunk Angiogenic Vessels

Multiphoton imaging of developing vessels in *TG(fli1:EGFP)*^{y1} morphants (A–D and F–K). Control (A, C, and F) and *plxnD1* (B, D, and G) morphants at approximately 24 hpf (A and B), 48 hpf (C, D, F, and G), and 3 dpf (H and I; see Supplemental Movies S3–S5). Control (J) and *sema3a2* (K) morphants at 48 hpf. Actin stress fibers in untreated HUVECs (L) collapse in response to application of Sema3A (M), as visualized by fluorescein-phalloidin staining. Sema3A-mediated inhibition of HUVEC migration (N) is partially suppressed by addition of VEGF (O). Semaphorin inhibits growth of intersegmental vessels. Confocal imaging of *TG(fli1:EGFP)*^{y1} embryos misexpressing either Sema3a2-V5-His (P–U, Y, and Z) or DsRed-Express (V–X). Panels show green fluorescent trunk vessels (P, S, and V), red construct-expressing cells (Q, T, and W) visualized by immunostaining of fixed animals (Q and T) or endogenous fluorescence in live animals (W), and corresponding merged images (R, U, and X). Intersegmental sprouts (arrows in [P]) are stalled adjacent to a large group of Sema3a2-V5-His expressing cells (P–R), but intersegmental vessels directly opposite them on the other side of the trunk of the same animal are growing normally (S–U). Intersegmental sprouts adjacent to a large group of cells expressing DsRed-Express are also not inhibited (V–X). Vessels grow indistinguishably in different regions of the trunk of a *plxnD1* morphant (Y and Z) with many (Y) or few (Z) Sema3a2-V5-His expressing cells, as visualized by immunohistochemistry for vascular EGFP (brown, arrows) and Sema3a2-V5-His (blue, arrowheads). Vessels are found in close apposition to groups of expressing cells (asterisk).

Images are lateral views, anterior to the left, except for (F) and (G), which show sagital reconstructions of the same image data used for (C) and (D). The shading in the diagram in (E) corresponds to the region of the trunk imaged in (F) and (G). Abbreviations in (E) are: NT, neural tube; No, notochord; M, myotomes/somites; DA, dorsal aorta; PCV, posterior cardinal vein. For 3D renderings of (A)–(D) and (H)–(K), see http://dir.nichd.nih.gov/Img/uvo/Plexin_3D.html. Scale bars = 50 μm (A–D, J, and K) and 50 μm (H and I).

al., 2001), which label the dorsal aorta and posterior cardinal vein, respectively. These three markers are expressed at equivalent levels in the blood vessels of uninjected animals, control morphants, and *plxnD1* morphants, confirming the lack of effects on endothelial cell differentiation upon loss of *plxnD1* function. Importantly, inspection of *plxnD1* morphants under transmitted light reveals no deficits in the patterning, size, or shape of nonvascular tissues (somites, notochord, brain, neural tube, etc.; data not shown) and immunocytochemistry

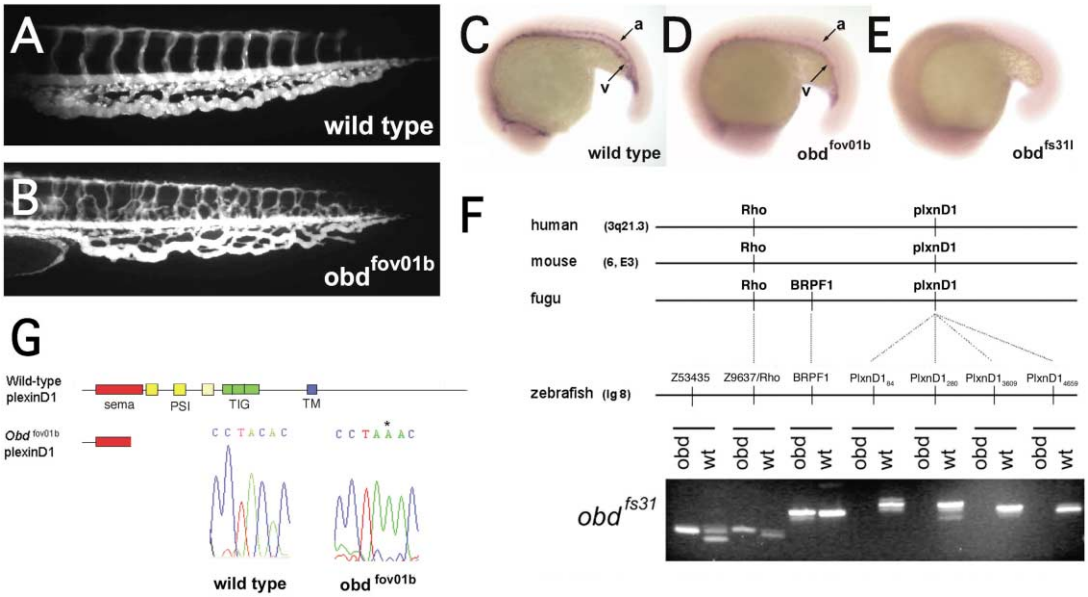

Figure 3. PlexinD1 Is Mutated or Absent in *out of bounds* Alleles

Angiography of 48 hpf wild-type (A) and *obd*^{fov01b} (B) embryos shows extensive mispatterning of trunk intersegmental vessels in *obd* mutants (lateral views of the tail, anterior to the left). In situ hybridization of *plexinD1* with 19 hpf embryos (C–E). *plxnD1* expression is clearly seen in the vein and artery of wild-type embryos (C), is reduced in *obd*^{fov01b} mutants (D), and is absent in *obd*^{fs31} mutants (E). Synteny among human, mouse, and fugu in the region of the closest markers to the *obd* locus was used to make new genetic markers despite the paucity of genomic sequence in the region. (F) *Peregrin (Brpf1)* and *plxnD1* are tightly linked to the locus by genetic mapping in the *obd*^{fs31} allele. Typing of four independent markers within the *plxnD1* locus (locations in the cDNA sequence are denoted in each marker name) demonstrates a genomic deletion of *plxnD1* in a pool of 24 *obd*^{fs31} mutants, but not in 24 of their wild-type siblings. Adjacent markers z53435, z9637, and *brpf1* are not deleted in *obd*^{fs31} mutants. Sequencing of *plxnD1* in a second mutant allele, *obd*^{fov01b}, revealed a stop codon at amino acid 318 resulting in a truncated protein with a partial semaphorin-like domain (G).

reveals normal neuronal patterns (see Experimental Procedures; data not shown). These results indicate that the function of *plxnD1* is endothelial specific, in agreement with its vascular-restricted expression.

out of bounds Mutants Exhibit Molecular Lesions in the *plxnD1* Gene

The defects observed in *plxnD1* morphants strongly resemble the phenotype of the recently described zebrafish mutant *out of bounds (obd)*, which exhibits virtually identical defects in intersegmental vessel formation and patterning (Figures 3A and 3B; Childs et al., 2002) and, like *plxnD1* morphants, specifically affects vascular tissues. The molecular basis of *obd* has not been previously determined, though a number of genes encoding candidate regulators of vascular patterning have been ruled out (Childs et al., 2002). Two alleles of *obd* are available, *obd*^{fov01b} and *obd*^{fs31}. *plxnD1* expression is reduced in *obd*^{fov01b} and undetectable in *obd*^{fs31} (Figures 3C–3E). Comparative radiation hybrid mapping of *plxnD1* and meiotic mapping of *obd* localize both to the same location at the bottom of linkage group 8 (see Experimental Procedures). Fine mapping and marker analysis reveals a complete deletion of *plxnD1* coding sequence in the *obd*^{fs31} allele, explaining the absence of *plxnD1* expression and indicating that this is a null mutation for *plxnD1* (Figure 3F). Since the *obd*^{fov01b} and *obd*^{fs31} alleles are phenotypically indistinguishable (Childs et al., 2002), this further suggests that *obd*^{fov01b} is likewise a functional null for *plxnD1*. Complete sequence analysis of *plxinD1* from *obd*^{fov01b} mutants and wild-type siblings reveals a single nucleotide change, a C to A transversion converting Tyr318 to a stop codon (Figure 3G). Translation of *plxnD1* from *obd*^{fov01b} would yield a truncated protein lacking the intracellular and transmembrane domains and most of the extracellular coding sequences including part of the semaphorin domain. It is possible that expression of this truncated, potentially diffusible protein might antagonize the function of the wild-type gene product (as in Takahashi and Strittmatter, 2001), perhaps explaining initial reports suggesting that *obd*^{fov01b} acts in a cell-nonautonomous fashion (Childs et al., 2002).

Several additional experiments to further verify the link between *obd* and *plxnD1* were also performed (see Supplemental Data). Technical limitations preclude successful phenotypic rescue of *obd* using *plxnD1* mRNA or DNA expression constructs (discussed in Supplemental Data), but injection of *plxnD1* morpholino into *obd* mutants results in no enhancement or alteration of the mutant phenotype. Together, our data conclusively show that defects in *plxnD1* are responsible for the *obd* mutant phenotype.

Reducing the Function of Type 3 Semaphorins Causes Vascular Patterning Defects

In the developing nervous system, plexins respond to semaphorin ligands expressed in adjacent tissues. One semaphorin, sema3A, has also been implicated in vascular development (Bates et al., 2003; Miao et al., 1999; Shoji et al., 2003). The zebrafish sema3A orthologs *sema3a1* and *sema3a2* are expressed in the developing

somites, but not in the intersomitic boundaries before and/or during the time of intersegmental vessel emergence and growth, suggesting that products of these genes might restrict the growth of these angiogenic sprouts. *sema3a1 (semaZ1a)* is expressed at 15 hpf in the entire somite, but from 18–36 hpf its expression is restricted to the dorsal and ventral portions of the myotomes, and it is excluded from the horizontal myoseptum (Yee et al., 1999). Misexpression experiments suggest *sema3a1*-mediated repulsion guides the lateral line growth cones through the horizontal myoseptum (Shoji et al., 1998) and inhibits angioblast migration (Shoji et al., 2003). *sema3a2 (semaZ1b)* is expressed throughout the somites at 14 hpf, becoming progressively restricted to newly formed posterior somites and to narrower bands of cells in the posterior half of the more anterior somites (Figures 1I and 1J), and its ectopic expression disturbs the pathfinding of ventral motor nerve branches (Roos et al., 1999). We used morpholinos to reduce the function of either *sema3a1* or *sema3a2* in *TG(fli1:EGFP)*^{y1} embryos, and observed intersegmental patterning defects qualitatively similar to those found in *plxnD1* morphants (Figures 2J and 2K; see Experimental Procedures). The defects were less frequent and less severe than those found in *plxnD1* morphants, likely reflecting semaphorin redundancy in the somites (*semaZ8* is also expressed in the somites in addition to *sema3a1* and *sema3a2* [Halloran et al., 1998]).

Type 3 Semaphorin-Mediated Endothelial Cell Repulsion Is *plxnD1* Dependent

In cultured human umbilical vein endothelial cells (HUVECs), which express *PLXND1*, addition of sema3A results in loss of actin stress fibers (Figures 2L and 2M, and see Experimental Procedures), a response associated with cell repulsion in plexin-expressing neurons (Tamagnone and Comoglio, 2000). This treatment also decreases endothelial cell migration in the absence or presence of vascular endothelial growth factor (VEGF) (Figures 2N and 2O), consistent with a direct effect of semaphorin signaling on endothelial cell migration. To establish an in vivo assay for inhibitory effects of type 3 semaphorins on the growth of intersegmental vessels, we used the *myogenin* (*myog*, Du et al., 2003) promoter to overexpress sema3a2 (or DsRed-Express, as a negative control) in somitic muscle of *TG(fli1:EGFP)*^{y1} embryos. Growth of intersegmental sprouts is inhibited adjacent to large groups of sema3a2-V5-His-expressing cells (Figures 2P–2R), but not elsewhere in the same animal where expressing cells are few in number or absent (Figures 2S–2U), or in control-injected animals adjacent to large numbers of cells expressing DsRed-Express (Figures 2V–2X). Inhibition of vessel growth is also not observed adjacent to cells expressing either DsRed-Express or Sema3a2-V5-His in *plxnD1* morphants, suggesting that without *plxnD1*, endothelial cells fail to sense the repelling signal provided by Sema3a ligands (Figures 2Y and 2Z).

Conclusions

Our results indicate that plexin signaling, crucial for regulating axonal pathfinding and neuronal patterning (Tamagnone and Comoglio, 2000), is also required for pathfinding and patterning of developing blood vessels (Figure 4). This work provides a molecular mechanism for the emerging view that the patterning of the earliest blood vessels is guided in large part by genetically programmed cues (Weinstein, 1999). Semaphorin effects on blood vessels and endothelial cells in vitro and in vivo have been described previously (Bates et al., 2003; Miao et al., 1999; Shoji et al., 2003), and our data support the requirement for semaphorin signaling during vascular patterning. Previously, these effects have been thought to result from an ability of semaphorins to compete with VEGF for neuropilin receptors (Bagnard et al., 2001; Bates et al., 2003; Miao et al., 1999; Shoji et al., 2003). In the nervous system, neuropilins are coreceptors with plexins for semaphorin ligands (Tamagnone and Comoglio, 2000; Gu et al., 2003), but in endothelial cells they have been shown to be important for VEGF signaling via the VEGF receptor Flk1 (Soker et al., 1998). Recent work indicates that neuropilins are, however, dispensable for semaphorin signaling during murine blood vessel patterning (Gu et al., 2003), suggesting that semaphorins may affect vascular development by mechanisms other than direct competition with VEGF, at least in mice. Our results demonstrate the requirement for functional PlexinD1 receptors during vascular patterning and suggest that previous interpretations of data regarding semaphorin signaling in endothelial cells need to be revisited in light of these new findings. Future studies will be needed to explore how repulsive sema3A signals interface within the endothelial cell with proangiogenic signals from VEGF and other factors.

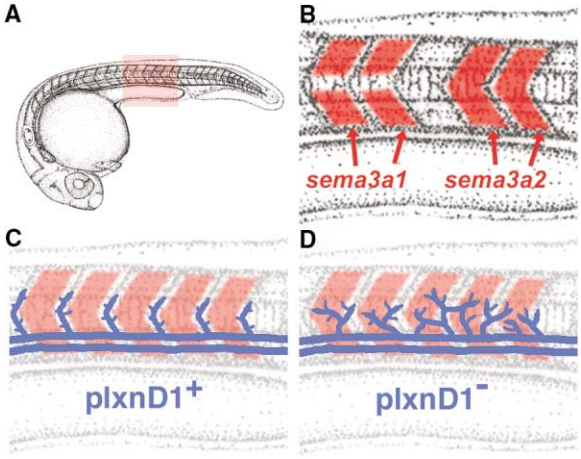

Figure 4. A Model for Regulation of Intersegmental Vascular Patterning in the Developing Trunk by Semaphorin-PlexinD1 Signaling

The central trunk region noted in (A) is shown at higher magnification in (B)–(D). Semaphorins *sema3a1* and *sema3a2* are expressed in the developing somites, but are excluded from intersomitic boundaries (B). PlexinD1-positive intersegmental vessel sprouts extend near to the semaphorin-free intersomitic boundaries but are restricted from growing away from these boundaries. (C). In *plxnD1* morphants or *obd* mutants, loss of PlexinD1 function allows vessels to grow into semaphorin-rich central regions of the somites (D).

Experimental Procedures

Cloning Zebrafish and Murine plxnD1 Genes

Using the cDNA sequence for human *PLXND1* (GenBank accession # AB014520), an orthologous zebrafish EST (GenBank accession # BI876917) was obtained by sequence comparison. A combination

of 5′ and 3′ RACE-PCR, cDNA cloning, and genomic sequence mining was used to obtain a full-length zebrafish sequence of 6474 nucleotides (GenBank accession # AY648302). A full-length murine *plxnD1* was isolated in parallel using similar methods (GenBank accession # XM_149784). See Supplemental Data, section 1, for additional information on comparative sequence analysis and RH mapping of zebrafish *plxnD1*.

Imaging and Expression Analysis

Videomicroscopic imaging and confocal or multiphoton imaging of *TG(fli1:EGFP)* zebrafish embryos were performed essentially as described (Lawson and Weinstein, 2002). Confocal microangiography was performed as described (Isogai et al., 2001). Zebrafish whole-mount RNA in situ hybridization was performed as described (Hauptmann and Gerster, 1994) using probes for *plxnD1*, *sema3A2*, *fli1*, *tie-1*, *ephrinB2*, and *ephB4*. Staining of trunk neuronal axons was performed using znp-1 (motor axon marker) and zn-12 (sensory neuron and lateral line marker) monoclonal antibodies as described (Trevarrow et al., 1990; Developmental Studies Hybridoma Bank). Expression of znp-1 and zn-12 at 24 and 32 hpf is identical in untreated embryos, control morphants, and *plxnD1* morphants. Somitic muscle expressing *sema3a2-V5-His* was detected immunochemically using a V5 monoclonal antibody (Invitrogen), an Alkaline Phosphatase Vectastain kit with either Vector Blue (Vector Laboratories) or fluorescent Fast Red (Roche Laboratories) substrates. Endothelial EGFP was detected using a polyclonal antibody (Clontech) and an HRP Vectastain kit using DAB substrate (Vector Laboratories).

Morpholino Oligonucleotide Injection

Morpholino oligonucleotides (morpholinos) were purchased from Gene Tools, LLC (see Supplemental Data, section 2 for sequences and specificities). Morpholinos were injected essentially as described previously (Lawson et al., 2002) into one-cell to four-cell *TG(fli1:EGFP)*^{y1} or *TG(fli1:nEGFP)* embryos (unpublished data). The following doses were injected per embryo in the described experiments: control 4.6, 7.5, or 10 ng; *plxnD1*$^{2215\text{-}2304}$ 4.6 ng; *plxnD1*$^{2215\text{-}2304}$ negative control 5 ng; *plxnD1*$^{3207\text{-}3462}$ 4.6 ng or 10 ng; *plxnD1*$^{3207\text{-}3462}$ negative control 10 ng; *sema3A1*$^{5'UTR}$ 5 ng; *sema3A1*$^{5'UTR}$ negative control 5 ng; *sema3A2*$^{560\text{-}670}$ 7.5 ng; *sema3A2*$^{560\text{-}670}$ negative control 7.5 ng. Morpholinos were tested over a range of doses and examined for specific and nonspecific phenotypes. In uninjected animals (n = 40, with 50–56 segments scored per embryo), no vascular patterning defects were observed. In control morphants (n = 15 embryos), 0.625% of the segments display ectopic or misguided vascular branches. In both *plxnD1* morphants, nearly 100% of segments were affected (n = 70 for each), while in *sema3A1*$^{5'UTR}$ (n = 27, 1146 segments) and *sema3A2*$^{560\text{-}670}$ (n = 28, 810 segments) morphants, 9.51% and 16.9% of the segments displayed intersegmental vessel patterning abnormalities, respectively. *sema3a1/sema3a2* double morphants are nonviable and thus were not analyzed. RT-PCR of the relevant *plxnD1* exons in gene targeting morphants reveals that levels of properly spliced mRNA are strongly reduced compared to control morphants (see Supplemental Data, section 2, for additional details). Importantly, morphants derived from injecting the cognate mismatch gene-specific control morpholinos for each of the four loss-of-function morpholinos used to reduce *plxnD1*, *sema3a*, and *sema3a2* activity displayed a wild-type vascular pattern: *plxnD1 2215-2304* negative control (n = 27), *plxnD1 3207-3462* negative control (n = 21), *sema3A1 5′UTR* negative control (n = 50), *sema3A2 560-670* negative control (n = 64).

Cell Culture Assays for Semaphorin Responses

Human umbilical vein endothelial cells (HUVEC; Clonetics) were grown in basic media (EBM, Clonetics) containing growth supplements (EGM), and were used for assays between passage 3 and 5. To test sema3A effects on the cytoskeleton, 1×10^6 HEK293T cells were transfected with 10 mg of pAG-Sema3A or pcDNA3.1, and the supernatants harvested 48 hr posttransfection. Separately, 2×10^5 HUVECs were plated in EGM onto glass coverslips. The next day, the medium was replaced with Sema3A-conditioned or control media and incubated 30 min at 37°C. Cells were fixed, and stained with fluorescein-phalloidin (Molecular Probes) to visualize filamentous actin and with DAPI to visualize nuclei. Collapse of the actin cytoskeleton is observed in greater than 95% of the cells, measured in five separate experiments with 100+ cells scored per experiment. Our negative control was conditioned media from mock-transfected cells. We verified specificity of Sema-conditioned media and calibrated potency using a growth cone collapse assay. In brief, dorsal root ganglia were explanted from chicken embryos and cultured in the presence of Sema-conditioned or mock-transfected media, and the ability of the conditioned media to collapse growth cones was assessed by light microscopy. Only the Sema-conditioned media produced growth cone collapse in this assay. To test sema3A effects on endothelial cell motility and migration, a Transwell migration apparatus (Costar; Cambridge, MA) with 8 mm pores coated with gelatin was used. To measure basal migration, 5×10^4 HUVECs in 120 ml EBM-0.2% BSA were loaded to the upper chamber, and 400 ml of either Sema3A-conditioned or control media was loaded into the lower chamber, and incubated for 4 hr at 37°C. To measure VEGF-stimulated migration, the experiment was performed as described, except 10 ng/ml VEGF was added to the bottom chamber. After incubation, cells were fixed and DAPI stained. Cells on the bottom surface of the membrane were counted in five random squares (0.5×0.5 mm).

Semaphorin Misexpression in Somitic Muscles

Muscle-specific misexpression of Sema3a2-V5-His or DsRed-Express (control) was performed by injecting 100–300 pg of either *myog:Sema3a2-V5-His* or *myog:DsRed-Express* vector DNA with or without *plxnD1*$^{3207\text{-}3462}$ morpholino (10 ng total) into *TG(fli1:EGFP)*^{y1} single-cell zebrafish embryos, and animals analyzed at 28–32 hpf. Misexpressing embryos were analyzed either by two color confocal imaging (visualization of vascular patterns, green; DsRed-Express or Sema3a2-V5-His, red) or immunochemically stained and scored under a stereomicroscope (vasculature, brown; Sema3a2-V5-His, blue). Embryos misexpressing DsRed-Express were anesthesized with Tricaine and imaged alive; *myog:Sema3a2-V5-His* injected animals were anesthesized, fixed, and fluorescently or chemically immunostained to visualize Sema3a2-V5-His expression.

Mapping and Positional Cloning of *Out of Bounds*

TL/WIK mapping crosses of *obd*^{fs31} and *obd*^{fov01b} (Childs et al., 2002) were prepared as described (Rawls et al., 2003). 1578 *obd*^{fs31} and 1424 *obd*^{fov01b} meioses were collected for mapping. Initial linkage using bulk segregant analysis placed *obd* 2 cm telomeric to the final map marker Z9637 on LG8. Nonchimeric YAC and BAC clones were unavailable in the region of interest, so we compared genes in the vicinity of *rhodopsin* (*Rho*) in other species. *Rhodopsin* has previously been mapped to Z9637 in zebrafish (www.zfin.org). Comparison of human, mouse, and Fugu genomes showed that *plexinD1 (plexnD1)* was linked in all three species. *Peregrin (Brpf1)* was also linked to *Rho* in Fugu. Radiation hybrid mapping on the LN54 panel (Hukriede et al., 2001) and further meiotic mapping confirmed that *Brpf1* was 0.3 cm (3/1128 meioses), *plxnD184* was 0.1 cm (1/1172 meioses), and *plxnD1465* and *plxnD16360* were 0 cm (0/1472 meioses) from the mutation in *obd*^{fov01b}. PCR with four independent primer pairs from *plexnD1* including exon and intron sequences shows complete deletion of *plexnD1* but not z9637 or *Brpf1* in *obd*^{fs31}. Sequencing of the complete *obd*^{fov01b} cDNA and relevant regions of *obd*^{fov01b} genomic DNA demonstrated a point mutation in an exon leading to the creation of a premature stop codon. Additional experiments aimed at further confirming the identity of *obd* with *plxnD1* are summarized in Supplemental Data, section 3).

Acknowledgments

We would like to thank Jonathan Epstein (Unit on Biologic Computation, NICHD) for assistance in implementing the website accompanying this paper. We would also like to thank Igor Dawid (Laboratory of Molecular Genetics, NICHD) for critical reading of this manuscript. We are very grateful to Harvey J. Pine and Daniel A. Castranova for excellent zebrafish care and to Dr. Sang-Yeob Yeo for graciously providing the neuronal antibodies used in this study and guidelines for their use. J.T.-V. is a Damon Runyon Fellow supported by the Damon Runyon Cancer Research Foundation (DRG-#1726-02).

A.D.G. is supported by an NIH predoctoral training grant to the University of Pennsylvania. S.D.F. is the recipient of a CIHR Strategic Training Program Fellowship in Genetics, Child Development, and Health. S.C. is supported by the Canadian Institutes for Health Research and is a Scholar of the Alberta Heritage Foundation for Medical Research and the Heart and Stroke Foundation of Canada. J.A.E. is supported by grants from the NIH and AHA. B.M.W. is supported by the Intramural Program of the National Institute of Child Health and Human Development.

Received: February 18, 2004
Revised: May 11, 2004
Accepted: May 11, 2004
Published online: June 10, 2004

References

Bagnard, D., Vaillant, C., Khuth, S.T., Dufay, N., Lohrum, M., Puschel, A.W., Belin, M.F., Bolz, J., and Thomasset, N. (2001). Semaphorin 3A-vascular endothelial growth factor-165 balance mediates migration and apoptosis of neural progenitor cells by the recruitment of shared receptor. J. Neurosci. *21*, 3332–3341.

Bates, D., Taylor, G.I., Minichiello, J., Farlie, P., Cichowitz, A., Watson, N., Klagsbrun, M., Mamluk, R., and Newgreen, D.F. (2003). Neurovascular congruence results from a shared patterning mechanism that utilizes Semaphorin3A and Neuropilin-1. Dev. Biol. *255*, 77–98.

Brown, L.A., Rodaway, A.R., Schilling, T.F., Jowett, T., Ingham, P.W., Patient, R.K., and Sharrocks, A.D. (2000). Insights into early vasculogenesis revealed by expression of the ETS-domain transcription factor Fli-1 in wild-type and mutant zebrafish embryos. Mech. Dev. *90*, 237–252.

Cheng, H.J., Bagri, A., Yaron, A., Stein, E., Pleasure, S.J., and Tessier-Lavigne, M. (2001). Plexin-A3 mediates semaphorin signaling and regulates the development of hippocampal axonal projections. Neuron *32*, 249–263.

Childs, S., Chen, J.N., Garrity, D.M., and Fishman, M.C. (2002). Patterning of angiogenesis in the zebrafish embryo. Development *129*, 973–982.

Draper, B.W., Morcos, P.A., and Kimmel, C.B. (2001). Inhibition of zebrafish fgf8 pre-mRNA splicing with morpholino oligos: a quantifiable method for gene knockdown. Genesis *30*, 154–156.

Du, S.J., Gao, J., and Anyangwe, V. (2003). Muscle-specific expression of myogenin in zebrafish embryos is controlled by multiple regulatory elements in the promoter. Comp. Biochem. Physiol. B Biochem. Mol. Biol. *134*, 123–134.

Gu, C., Rodriguez, E.R., Reimert, D.V., Shu, T., Fritzsch, B., Richards, L.J., Kolodkin, A.L., and Ginty, D.G. (2003). Neuropilin-1 conveys semaphorin and VEGF signaling during neural and cardiovascular development. Dev. Cell *5*, 45–57.

Halloran, M.C., Severance, S.M., Yee, C.S., Gemza, D.L., and Kuwada, J.Y. (1998). Molecular cloning and expression of two novel zebrafish semaphorins. Mech. Dev. *76*, 165–168.

Hauptmann, G., and Gerster, T. (1994). Two-color whole-mount in situ hybridization to vertebrate and *Drosophila* embryos. Trends Genet. *10*, 266.

Hukriede, N., Fisher, D., Epstein, J., Joly, L., Tellis, P., Zhou, Y., Barbazuk, B., Cox, K., Fenton-Noriega, L., Hersey, C., et al. (2001). The LN54 radiation hybrid map of zebrafish expressed sequences. Genome Res. *11*, 2127–2132.

Isogai, S., Horiguchi, M., and Weinstein, B.M. (2001). The vascular anatomy of the developing zebrafish: an atlas of embryonic and early larval development. Dev. Biol. *230*, 278–301.

Lawson, N.D., and Weinstein, B.M. (2002). In vivo imaging of embryonic vascular development using transgenic zebrafish. Dev. Biol. *248*, 307–318.

Lawson, N.D., Scheer, N., Pham, V.N., Kim, C.H., Chitnis, A.B., Campos-Ortega, J.A., and Weinstein, B.M. (2001). Notch signaling is required for arterial-venous differentiation during embryonic vascular development. Development *128*, 3675–3683.

Lawson, N.D., Vogel, A.M., and Weinstein, B.M. (2002). sonic hedgehog and vascular endothelial growth factor act upstream of the Notch pathway during arterial endothelial differentiation. Dev. Cell *3*, 127–136.

Lyons, M.S., Bell, B., Stainier, D., and Peters, K.G. (1998). Isolation of the zebrafish homologues for the tie-1 and tie-2 endothelium-specific receptor tyrosine kinases. Dev. Dyn. *212*, 133–140.

Miao, H.Q., Soker, S., Feiner, L., Alonso, J.L., Raper, J.A., and Klagsbrun, M. (1999). Neuropilin-1 mediates collapsin-1/semaphorin III inhibition of endothelial cell motility: functional competition of collapsin-1 and vascular endothelial growth factor-165. J. Cell Biol. *146*, 233–242.

Rawls, J.F., Frieda, M.R., McAdow, A.R., Gross, J.P., Clayton, C.M., Heyen, C.K., and Johnson, S.L. (2003). Coupled mutagenesis screens and genetic mapping in zebrafish. Genetics *163*, 997–1009.

Risau, W., and Flamme, I. (1995). Vasculogenesis. Annu. Rev. Cell Dev. Biol. *11*, 73–91.

Roos, M., Schachner, M., and Bernhardt, R.R. (1999). Zebrafish semaphorin Z1b inhibits growing motor axons in vivo. Mech. Dev. *87*, 103–117.

Shoji, W., Yee, C.S., and Kuwada, J.Y. (1998). Zebrafish semaphorin Z1a collapses specific growth cones and alters their pathway in vivo. Development *125*, 1275–1283.

Shoji, W., Isogai, S., Sato-Maeda, M., Obinata, M., and Kuwada, J.Y. (2003). Semaphorin3a1 regulates angioblast migration and vascular development in zebrafish embryos. Development *130*, 3227–3236.

Soker, S., Takashima, S., Miao, H.Q., Neufeld, G., and Klagsbrun, M. (1998). Neuropilin-1 is expressed by endothelial and tumor cells as an isoform-specific receptor for vascular endothelial growth factor. Cell *92*, 735–745.

Takahashi, T., and Strittmatter, S.M. (2001). Plexina1 autoinhibition by the plexin sema domain. Neuron *29*, 429–439.

Tamagnone, L., and Comoglio, P.M. (2000). Signalling by semaphorin receptors: cell guidance and beyond. Trends Cell Biol. *10*, 377–383.

Tamagnone, L., Artigiani, S., Chen, H., He, Z., Ming, G.I., Song, H., Chedotal, A., Winberg, M.L., Goodman, C.S., Poo, M., et al. (1999). Plexins are a large family of receptors for transmembrane, secreted, and GPI-anchored semaphorins in vertebrates. Cell *99*, 71–80.

Tessier-Lavigne, M., and Goodman, C.S. (1996). The molecular biology of axon guidance. Science *274*, 1123–1133.

Trevarrow, B., Marks, D.L., and Kimmel, C.B. (1990). Organization of hindbrain segments in the zebrafish embryo. Neuron *4*, 669–679.

van der Zwaag, B., Hellemons, A.J., Leenders, W.P., Burbach, J.P., Brunner, H.G., Padberg, G.W., and Van Bokhoven, H. (2002). PLEXIN-D1, a novel plexin family member, is expressed in vascular endothelium and the central nervous system during mouse embryogenesis. Dev. Dyn. *225*, 336–343.

Weinstein, B.M. (1999). What guides early embryonic blood vessel formation? Dev. Dyn. *215*, 2–11.

Yee, C.S., Chandrasekhar, A., Halloran, M.C., Shoji, W., Warren, J.T., and Kuwada, J.Y. (1999). Molecular cloning, expression, and activity of zebrafish semaphorin Z1a. Brain Res. Bull. *48*, 581–593.